



Provided by the author(s) and University of Galway in accordance with publisher policies. Please cite the published version when available.

Title	Cyclic loading tests on sandstone and limestone shale aggregates used in unbound forest roads
Author(s)	Rodgers, Michael; Hayes, G; Healy, Mark G.
Publication Date	2009
Publication Information	Rodgers, M., Hayes, G., and Healy, M.G. (2009) 'Cyclic loading tests on sandstone and limestone shale aggregates used in unbound forest roads'. Construction and Building Materials, 23 :2421-2427.
Publisher	Elsevier
Link to publisher's version	<a href="http://dx.doi.org/10.1016/j.conbuildmat.2008.10.007">http://dx.doi.org/10.1016/j.conbuildmat.2008.10.007</a>
Item record	<a href="http://hdl.handle.net/10379/2913">http://hdl.handle.net/10379/2913</a>
DOI	<a href="http://dx.doi.org/10.1016/j.conbuildmat.2008.10.007">http://dx.doi.org/10.1016/j.conbuildmat.2008.10.007</a>

Downloaded 2024-03-20T11:56:06Z

Some rights reserved. For more information, please see the item record link above.



CYCLIC LOADING TESTS ON SANDSTONE AND LIMESTONE SHALE  
AGGREGATES USED IN UNBOUND FOREST ROADS

M. Rodgers\*, G. Hayes and M.G. Healy

Department of Civil Engineering, National University of Ireland, Galway, Ireland.

\* Corresponding author. E-mail: michael.rodgers@nuigalway.ie. Tel: +353 91 492219;

Fax: +353 91 494507.

**Published as: Rodgers, M., Hayes, G., Healy, M.G. 2009. Cyclic loading tests on sandstone and limestone shale aggregates used in unbound forest roads. Construction and Building Materials 23: 2421 – 2427.**

**Abstract**

This study examined the performance of two aggregates subjected to cyclic loading in a large-scale test rig. The two aggregates examined were: (i) a sandstone from Co. Cork, Ireland and (ii) a limestone shale from Co. Limerick, Ireland. The aggregates were classified and their engineering properties established and compared. Various depths of the aggregates, overlaying a 1 m-deep formation layer, were compacted and subjected to a cyclic loading regime of incrementally increasing pressures of 500 kPa, 750 kPa and 1,000 kPa. Each aggregate was tested for up to 150,000 load applications. The resilient pressures, resilient surface deflections and permanent deformations were measured. The sandstone performed well in a dry state but poorly when wetted up. The shale behaved poorly but the addition of a wet mix macadam (WWM) layer greatly improved its performance.

*Keywords:* unbound forest road; cyclic loading; sandstone; limestone shale; aggregate.

## **Introduction**

Unbound forest roads must have low construction and maintenance costs. These low costs are a necessary requirement due to the limited value of the timber resource and the timescale involved between productive outputs. As a result, cheap road aggregates are sought after, which must be capable of sustaining the loads imposed by heavy forest trafficking. The aggregates must have adequate resistance to weathering, abrasion and erosion, and have adequate bonding to resist dislodging.

In road construction, it is the resistance to permanent deformation rather than the strength of the road material that is of importance. Resistance to deformation is achieved using dense, well-graded materials (Brown, 1981; Shen et al., 2005). High permeability, high elastic stiffness and low variability are the major requirements for granular materials used in road construction.

In unbound forest roads constructed from granular material, repeated wheel loading can cause shearing of the materials that results in permanent deformations. Rutting is the cumulative vertical compression that occurs if the compressive strains are irrecoverable after the removal of the wheel load. A maximum permissible rut depth of between 40 mm (Powell et al., 1984) and 75 mm (Giroud and Han, 2004) is commonly used to classify pavement failure. Rutting at the surface is associated with rutting at the aggregate-soil

interface. The rut depth,  $s$  (mm), may be calculated for geosynthetic, reinforced pavements from (Giroud and Han, 2004):

$$s = \frac{\frac{P}{\pi r^2} f_s}{\left[ \frac{h + 0.204h(R_E - 1)}{0.868r + r(0.661 - 1.006J^2) \left(\frac{r}{h}\right)^{1.5} \log N} + 1 \right]^2 \left[ \left[ 1 - 0.9 \exp \left[ - \left(\frac{r}{h}\right)^2 \right] \right] N_c c_u \right]} \quad (1)$$

where  $J$  is the aperture stability modulus of the geogrid ( $\text{m N}^0$ );  $r$ , the radius of the equivalent tire contact area (m);  $h$ , the depth of the completion layer (m);  $N$ , the number of loading cycles;  $P$ , the wheel load (kN),  $N_c$ , the bearing capacity factor;  $f_s$ , the maximum allowable rut depth (75mm); and  $c_u$ , the undrained cohesion of the formation layer (kPa). The limited modulus ratio,  $R_E$ , can be calculated from (Giroud and Han, 2004):

$$R_E = \min \left( \frac{E_{cl}}{E_{fl}}, 5.0 \right) = \min \left( \frac{3.48 CBR_{cl}^{0.3}}{CBR_{fl}}, 5.0 \right) \quad (2)$$

where  $E_{cl}$  and  $E_{fl}$  are the completion layer and formation layer resilient moduli, respectively (kPa), and  $CBR_{cl}$  and  $CBR_{fl}$  are the California Bearing Ratios of the completion layer and formation layer aggregates, respectively (%).

The objectives of this study were:

1. To design and build a cyclic load testing machine.
2. To classify sandstone and limestone shale aggregates that are used in Irish unbound forest roads, and to monitor their performance in the cyclic load testing rig.

## **Materials and Methods**

### *Aggregate classification tests*

The two completion materials examined were a good quality sandstone aggregate and a poor quality limestone shale aggregate. The sandstone aggregate originated from arenaceous sedimentary rock. It was non-calcareous, non-clayey and siliceous. The second completion aggregate – limestone shale - was also sedimentary but argillaceous in origin.

Aggregate samples were collected and stored in sealed bags. Excessively large particles (> 50 mm) were removed to aid compaction and the optimal water content (OWC) was determined using the Proctor test (BS 1377, Part 4, 1990).

### *Placement of materials and instrumentation*

The formation material was dried below the OWC and was compacted in 50 mm layers in a 1.2 m x 1.2 m bin, using a vibrating hammer fitted with a 150 mm square plate. The

appropriate mass of water was added to each sample to increase the water content to its OWC ( $13.5 \% \pm 0.5\%$ ). The formation material was built to a 1000 mm depth and was then left for three days for its water content to equilibrate. The completion layer aggregates were placed on top of the formation material. *In-situ* dry density and water content in the layers were monitored using a nuclear density probe.

Four 100 mm-diameter pressure cells measured the resilient pressure due to the applied load in the formation material and were placed at heights of 300, 500, 700 and 900 mm above the bin base as the soil was compacted (Figure 1). Two large-range pressure cells (0-10 bar) were placed towards the top of the formation layer and low range pressure cells (0-5 bar and 0-2 bar) were placed towards the bin base. They operated on a 10 V D.C. input with a 0 - 100 mV output. Linear strain conversion transducers (lscts) (MPE Transducers Ltd., UK), as well as two standard dial gauges, monitored the resilient deflections – the deflection due to load application - and permanent deformation of the completion aggregate along the central line of the loading pad. The lscts were calibrated using a micrometer block and a computer software package (LabVIEW™, National Instruments Ltd., Austin, USA) before use. The dial gauges were capable of measuring to 0.01 of a millimetre.

LabVIEW™ was used to log the data from the transducers and pressure cells. The LabVIEW™ program was used in conjunction with an NB - M10 - 16L -9 analog to digital (A/D) board, which had the capacity to log up to 8 separate input channels.

### *Loading rig construction*

A cyclic-load testing machine was designed and constructed to apply pressures, similar to that of a truck tyre, to the aggregate materials (Figure 1). The loading frame comprised two simply supported universal beams (Steel Grade 43) constructed in parallel on common steel base-plates. 305 x 165 UB 40 sections were used for both the beams and columns. 2 No. 700 x 700 mm holes were broken out of the existing concrete floor and 8 No. M20 Gr. 8.8 x 180 bolts were sunk to a depth of 140 mm in a 200 mm depth of C40 concrete (28 day strength =  $40 \text{ N mm}^{-2}$ ) to provide a suitable reaction for the base-plates of the frame. Flat strips of metal were welded to the ends of the bolts to ensure complete grip in the concrete.

The loading pad comprised a 45 mm-thick, tyre grade, rubber pad (Dunlop, England), 200 mm in diameter, bonded to a 10 mm-deep steel plate. The plate was fixed to a steel frame and a universal joint - positioned at the end of an actuator piston - to ensure uniform contact between the pad and the aggregate surface during testing. Incremental pressure loads were applied to the aggregate using a hydraulic actuator (Pressure Hydraulics Ltd., UK) with a 40 kN loading capacity. The actuator was calibrated using a proving ring and was controlled by a programmable servo amplifier. A loading cycle, 3 seconds in duration, comprised 1 second of loading and 2 seconds of recovery. The loading cycles were as follows:

$50 \times 10^3$  cycles at an applied pressure of 500 kPa.

50x10<sup>3</sup> cycles at an applied pressure of 750 kPa.

50x10<sup>3</sup> cycles at an applied pressure of 1000 kPa.

Six full-scale tests were performed on the aggregates and are listed in Table 1. Surface deformations of the completion layer and resilient pressures in the formation layer were measured during the cyclic loading for the following road structure arrangements and conditions: (i) 150 mm and 250 mm-deep layers of sandstone, and 250 mm and 400 mm-deep layers of limestone shale completion materials; (ii) the effect of water addition to the surface of the 150 mm-deep sandstone; and (iii) capping of the 250 mm-deep limestone shale layer with 100 mm and 200 mm-deep layers of Clause 810 wet mix macadam (WMM). Test 1 was carried out on the sandstone compacted to a depth of 250 mm in 5 layers, at an average water content (WC) of 3.4±0.3 % per layer. In Test 2, 150 mm-deep sandstone was compacted in 3 layers at an average WC of 3.5±0.2 %. After completion of 150x10<sup>3</sup> cycles, 10 mm of water was sprayed onto the aggregate surface and was allowed to soak for one hour. The test was then restarted at an applied pressure of 500 kPa and run for 4x10<sup>3</sup> loading cycles. In Test 3, 250 mm-deep shale was compacted in 5 layers at an average WC of 7.5±0.2 %. In Test 4, 400 mm-deep shale was compacted at a WC of 7.2±0.3% in 3 layers. In Test 5, 200 mm-deep Clause 810 WMM overlaid 250 mm-deep shale. The shale was compacted at 7.0% WC and the overlying WMM was then compacted at an average WC of 2.7%. Test 6 - 100 mm-deep WMM over 250 mm-deep shale - was compacted in a similar manner to Test 5. During each loading cycle, the resilient pressure and deflection, and permanent deformation were measured. Following completion of each test and removal of the aggregate, the top 50



mm layer of the formation material was removed and fresh soil compacted into the bin at the OWC. A previous study on a similar completion material, 150 mm deep, which was subjected to  $50 \times 10^3$  cycles at 500 kPa, followed by  $50 \times 10^3$  cycles at 750 kPa and  $50 \times 10^3$  cycles at 1000 kPa, resulted in little deformation in the formation material (about 2 mm) at higher maximum resilient pressures (Kielty, 1997). As the formation material was compacted in 50 mm layers, it was considered adequate to remove only the top 50 mm layer.

## **Results and Discussion**

### *Aggregate classification tests*

Classification tests, including tests for natural water content, Atterberg limits, specific gravity and particle size distribution, were carried out on both the formation and the completion materials in accordance with the British Standards.

The strength of the completion layer aggregates was also tested using the CBR test (BS 1377, Part 4, 1990), the Aggregate Impact Value (AIV, BS 812, Part 112, 1990), the Aggregate Crushing Value (ACV, BS 812, Part 110, 1990), the Aggregate Abrasion Value (AAV, BS 812, Part 113, 1990), and the 10% Fines Value (TFV, BS 812, Part 111, 1990). The CBR test compares the bearing capacity of a material with that of a well-graded crushed stone. Completion layer materials should have CBR values greater than 30% for roads expected to carry more than 0.5 million standard axles. For less heavily trafficked roads, a CBR greater than 20% is necessary. The AIV gives a relative measure

of an aggregate's resistance to sudden shock loading and an AIV < 35% is recommended. The ACV is a measure of the relative resistance to a gradually applied compressive load. A limit of 35% is recommended. The AAV gives an indication of an aggregate's resistance to surface abrasion. The test reflects the hardness of the aggregate's constituent minerals, the influence of cleavage and the intergranular bonding, all of which are important factors regarding an aggregate's ability to resist degradation.

Durability - a measure of an aggregate's resistance to environmental influences like wetting, thermal expansion/contraction and freeze/thaw effects - was tested using the magnesium sulphate soundness value (MSSV) test and the water absorption value (WAV) test. The cohesive strength of the formation material,  $c_u$ , was determined from the direct shear test (BS 1377, Part 8, 1990).

The aggregate was a well-graded formation soil (Figure 2). The sandstone and the shale were both poorly graded. Table 2 lists the values obtained from the laboratory testing of the aggregates. The sandstone satisfies the 30% CBR limit but the shale fails the CBR test. The shale also had a poor MSSV while the sandstone was quite 'sound' and was well above the 75 % limit. The results for dry and wet AIV tests on each aggregate are below the limits (< 35 % dry and < 40 % soaked). The sandstone had the greatest resistance to abrasion and was well below the limit.

*Resilient pressures*

In Test 1 (250 mm-deep sandstone), at an applied pressure of 500 kPa, the pressure in Cell D – 900 mm from the base of the bin – reduced from 36 kPa to 28 kPa (Figure 3). During the subsequent applied pressures of 750 kPa and 1000 kPa, the resilient pressure increased to 59 kPa and 62 kPa, respectively. In Test 2, reducing the aggregate depth to 150 mm increased the resilient pressure in Cell D. At the beginning of the first loading cycle, the resilient pressure dropped from 82 kPa to 70 kPa. At applied pressures of 750 kPa and 1000 kPa, the resilient pressure increased to 104 kPa and 132 kPa, respectively. After the application of 10 mm of rainfall, the test was restarted at an applied pressure of 500 kPa. The test was stopped after  $4 \times 10^3$  loading cycles due to excessive permanent deformation. During this loading cycle, the resilient pressure increased from 116 to 117 kPa. In Test 3, 250 mm-deep limestone shale produced greater residual pressures in Cell D. At the end of  $50 \times 10^3$  loading cycles, the residual pressure at Cell D was 47 kPa – 39% greater than the residual pressure measured in the 250 mm-deep sandstone at the same pressure. Testing was suspended after  $50 \times 10^3$  loading cycles due to the excessive permanent deformation of 10.2 mm. In Test 4, approximately the same residual pressures were measured in Cell D and the test was suspended after  $50 \times 10^3$  loading cycles due to excessive permanent deformation. In Test 5, a 200 mm-deep WMM capping layer placed on top of 250 mm-deep limestone shale improved its performance. Residual pressures lower than all other aggregates were measured under all applied pressures. In Test 6, reducing the WMM capping layer to 100 mm over the same depth of limestone shale, increased the resilient pressures at all applied loads. At  $50 \times 10^3$ ,  $100 \times 10^3$  and  $150 \times 10^3$  cycles, resilient pressures were 33, 40 and 29% greater than the equivalent resilient pressures measured at the same number of loading cycles using 200 mm-deep WMM

over limestone shale, but were comparable with those of the 250 mm-deep sandstone performance.

### *Resilient deflections*

In Test 1, the resilient deflections ranged from 0.7 – 1.2 mm during application of 500 kPa and 1000 kPa loading pressures. By reducing the sandstone depth to 150 mm in Test 2, the resilient deflections increased by 47%, 15% and 29% over the values measured at the equivalent loading pressures in Test 1. The addition of water to the sandstone had a significant effect on its resilient deflection. Over  $4 \times 10^3$  loading cycles, at the 500 kPa pressure, the resilient deflections rose from 1.0 mm to 1.5 mm. In Tests 3 and 4, 250 mm-deep and 400 mm-deep limestone shale produced maximum resilient deflections of 1.0 mm at an applied pressure of 500 kPa. In both tests, loading was suspended due to high permanent deformations. The addition of a 200 mm-deep (Test 5) and 100 mm – deep (Test 6) WWM capping layers on 250 mm-deep limestone shale produced the best results from the study. In Test 5, maximum resilient deflections of 0.3, 0.4 and 0.6 mm were measured at loading pressures of 500, 750 and 1000 kPa, respectively. In Test 6, under a reduced WMM aggregate depth of 100 mm, resilient deflections of 0.5, 0.7 and 0.9 mm were measured at similar applied loading pressures; these deflections were lower than for the sandstone.

### *Permanent deformations*

In Test 1, a total permanent deformation of 2.9 mm was recorded in the 250 mm-deep sandstone after  $150 \times 10^3$  loading cycles (Figure 5). 60% of this deformation occurred after 1000 loading cycles at an applied pressure of 500 kPa. In Test 2, at a reduced aggregate depth of 150 mm, a similar permanent deformation was measured after  $150 \times 10^3$  loading cycles. The addition of water to the aggregate produced a permanent deformation of 15 mm after 3000 cycles at an applied pressure of 500 kPa. In Test 3, 89% of the total permanent deformation – about 9 mm - in the 250 mm-deep limestone shale occurred within 250 cycles at an applied pressure of 500 kPa. After application of an applied pressure of 750 kPa for 250 cycles, the permanent deformation was 10.2 mm and the test was stopped. This was to prevent damage to the hydraulic actuator. A similar result was recorded in Test 4 using a 400 mm-deep limestone shale. A maximum permanent deformation of 4.1 mm was recorded at  $50 \times 10^3$  loading cycles but after 200 cycles at an applied pressure of 750 kPa, the permanent deformation reached 13.2 mm and the test was suspended. The best results for the two aggregates were produced by capping a 250 mm-deep limestone shale with 200 mm-deep WMM. After  $150 \times 10^3$  loading cycles, the total permanent deformation measured was 0.85 mm – up to 70% less than the previous aggregates tested under the same number of loading cycles. In Test 6, the reduction in aggregate depth to 100 mm produced a total permanent deformation of 1.7 mm.

#### *Prediction of rut depths under cyclic loadings*

Eqn. 1 was used to compare the theoretical rut depth,  $s$ , with the measured rut depth. As the aggregates were un-reinforced and unpaved,  $J = 0$  and  $N_c = 3.14$  (Giroud and Han,

2004). The radius of the tire contact area,  $r$ , was 0.1m. As Eqn. 1 is only valid for  $CBR_{\text{fi}}$  ratios less than or equal to 5 (Giroud and Han, 2004), the  $E$ -values of the formation and completion layers were used to calculate  $R_E$ . The  $E$ -values were selected by calibrating a finite element model for stress and deformation analysis of earth structures (SIGMA/W, GEO-SLOPE International Ltd., Alberta, Canada). These selections were made when the predicted resilient deflection was equal to the experimental value under the centre of the loading pad for the same applied pressure. SIGMA/W contains three separate programs, Define, Solve and Contour. The Define program sets up the problem by drawing the system geometry and inputting the soil characteristics and loading values. The Solve program is used to compute the deformations and stress changes. The Contour program graphs the computed parameters. SIGMA/W comprises eight elastic and plastic constitutive soil models, all of which may be applied to two-dimensional plane strain and axisymmetric problems. The model selected to conduct the analysis was dictated by the experimental results.

All the materials tested showed signs of plastic behaviour due to their continual increase in permanent deformation with increasing number of loading cycles (Figure 5). The elastic-plastic SIGMA/W model was therefore used for modelling the experimental results. The  $E$  values obtained by calibrating the finite element model, SIGMA/W, are given in Table 3. These values were used to predict the rut depths – permanent deformations - using Eqn. 1 (Table 4). The rut depths at three cycles - 50,000, 100,000 and 150,000 - were examined. The effectiveness of Eqn. 1 in predicting rut depths is dependent on: (i) the measured undrained cohesion of the formation soil and (ii) the  $E$

values of the formation and completion materials, estimated from SIGMA/W. In this study, the calculated values of the permanent deformations were, in general, of the same order as those measured in the loading rig (within 3 mm), except for (i) the 0.4 deep limestone shale layer after  $50 \times 10^3$  loading cycles at 500 kPa, and (ii) the 0.15 m deep sandstone layer after  $50 \times 10^3$  cycles at 500 kPa, followed by  $50 \times 10^3$  cycles at 750 kPa and  $50 \times 10^3$  cycles at 1000 kPa.

## **Conclusions**

From the large-scale cyclic loading tests, the following conclusions were made:

1. The sandstone had very good resistance to deformation in a dry state and was able to withstand high applied pressures, up to 1,000 kPa, without excessive rutting.
2. Simulated rainfall of 10 mm had the effect of causing increased rutting in the sandstone aggregate and increased stresses in the subgrade soil.
3. The shale had poor resistance to rutting but the addition of a WMM layer greatly improved its performance.
4. The sandstone is a better roadbase material than the shale.

## **Acknowledgements**

This project, was funded by the National Council for Forest Research and Development (COFORD), the European Union (EU) and the Irish Forestry Board (Coillte Teoranta), under Section 3, Harvesting and Transport, of the Forestry Research Programme, 1994 -

1999. The authors acknowledge the help of Mr. Tom Ryan and Mr. Peter Fee of Coillte Teoranta.



## References

- [1] Browne SF. The structural role of granular materials in flexible pavements. In: Jones, R.H. (editor). Symposium on unbound aggregates in roads, 1981.
- [2] B.S. 1377: Part 4. Methods for determination of California Bearing Ratio (CBR). British Standards Institution, London, 1990.
- [3] B.S. 1377: Part 8. Methods of test for soils for civil engineering purposes – shear strength tests (effective stress). British Standards Institution, London, 1990.
- [4] B.S. 1377: Part 9. Compaction test. British Standards Institution, London, 1990.
- [5] B.S. 812: Part 110. Method of determination of the aggregate crushing value (ACV). British Standards Institution, London, 1990.
- [6] B.S. 812: Part 111. Methods for determination of ten per cent fines value (TFV). British Standards Institution, London, 1990.
- [7] B.S. 812: Part 112. Methods for determination of aggregate impact value (AIV). British Standards Institution, London, 1990.
- [8] B.S. 812: Part 113: Method of determination of aggregate abrasion value (AAV). British Standards Institution, London, 1990.
- [9] Giroud JP, Han J. Design method for geogrid-reinforced unpaved roads. II. Calibration and applications. J Geotech Geoenviron Eng 2004; 130 (8): 787 – 797.

- [10] Kielty A. A comparative study on the behaviour of two aggregates under repeated loading. M.Eng.Sc. thesis submitted to the National University of Ireland, Galway, 1997.
- [11] Powell WD, Potter JF, Mayhew HC, Nunn ME. The structural design of bituminous roads. Laboratory report LR 1132. TRRL, Crowthorne, 1984.
- [12] Shen D-H, Kuo M-F, Du J-C. Properties of gap-aggregate gradation asphalt mixture and permanent deformation. Constr Build Mater 2005; 19(2): 147-153.

## **List of figures**

Figure 1. The laboratory loading apparatus.

Figure 2. Particle size distributions for the materials.

Figure 3. Resilient pressures, measured 900 mm from the base of the formation layer, versus number of cycles.

Figure 4. Maximum resilient deflections measured at the surface of the completion layer versus number of cycles.

Figure 5. Maximum permanent deformations measured at the surface of the completion layer versus number of cycles.

Table 1. List of full-scale tests.

Test no.	Material	Thickness <sup>†</sup> mm	Optimum water content %	Initial water content %	Final dry density Mg m <sup>-3</sup>
1	Sandstone	250	5.5	3.4± 0.3	1.93± 0.02
2	Sandstone	150	5.5	3.5± 0.2	1.88± 0.04
3	Limestone shale	250	12.0	7.5% ± 0.2	1.61± 0.02
4	Limestone shale	400	12.0	7.2% ± 0.3	1.64± 0.01
5	Clause 810 over Limestone shale <sup>‡</sup>	200+250	-	-	-
6	Clause 810 over Limestone shale	100+250	-	-	-

<sup>†</sup> Thickness refers to the completion layer. The formation material had a thickness of 1000 mm for all tests.

<sup>‡</sup> 200 mm of a crushed limestone graded to the specification of a wet mix macadam (WMM) was compacted, at a water content of 3.3 %, onto a 250 mm layer of the limestone shale.

Table 2. Summary of BS laboratory test results.

Laboratory tests	Limits	Formation	Completion Sandstone	Limestone shale	Clause 810
Natural water content (%)	-	21.5	-	-	
Liquid limit	-	32.3	30	36	
Plastic limit (%)	-	23	Non plastic	21	
Plasticity index (%)	0-6	9.7	0	15	
Specific gravity (Gs)	-	2.07	2.69	2.64	
Max. dry density (Mg m <sup>-3</sup> )	-	1.8	2.0	2.1	
Optimum water content (%)	-	13.5	5.5	12.0	
California bearing ratio (%)*	2/30	15.0	37	<17	
Flakiness index (%)	<35.0	-	32.0	37.0	
MSSV (%)	>75.0	-	86.4	1.1	
Water absorption value (%)	<2.0	-	2.9	6.2	
Dry aggregate crushing value (%)	<35.0	-	22	37	21
Wet aggregate crushing value (%)	-	-	25	36	23
Dry aggregate impact value (%)	<35.0	-	17	27	15
Wet aggregate impact value (%)	<40.0	-	20	29	16
Aggregate abrasion value (%)	<10.0	-	5.3	43.9	11
Effective size, d <sub>10</sub> , (mm)		3.9x10 <sup>-3</sup>	1.7x10 <sup>-1</sup>	5.5	
Uniformity coefficient, C <sub>u</sub>		44.9	19.8	5.7	

\* The minimum allowable *in situ* CBR for a subgrade soil is 2%.

Table 3. Estimation of resilient moduli.<sup>†</sup>

Test	Material	Thickness	Applied pressure (kPa)		
		m	500	750	1000
			Calculated resilient moduli, E (MPa)		
	Formation	1	37	37	37
1	Sandstone	0.25	205	160	170
2	Sandstone	0.15	220	164	214
3	Limestone shale	0.25	105	-	-
4	Limestone shale	0.40	105	-	-
5	Clause 810 over limestone shale	0.2 + 0.25	455	535	550
6	Clause 810 over limestone shale	0.1 + 0.25	335	340	375

<sup>†</sup> The resilient moduli for the soils were estimated by calibrating the SIGMA/W finite element model of the soils and loadings to provide resilient deflections under the centre of the loading pad that were equal to the experimental results.

Table 4. Comparison of modelled versus measured rut depths.

Test	Material	Thickness	No. of cycles								
			0-50,000 at 500 kPa		0-50,000 at 500 kPa		0 - 50,000 at 500 kPa				
					50,000 – 100,000 kPa		50,000 – 100,000 at 750 kPa				
							100,000 – 150,000 at 1000 kPa				
							rut depth, s				
						Calculated	Measured	Calculated	Measured	Calculated	Measured
m			mm	mm	mm	mm	mm	mm			
	Formation	1	-	-	-	-	-	-			
1	Sandstone	0.25	1.1	2.4	2.8	2.8	4.7	2.9			
2	Sandstone	0.15	2.0	1.5	4.6	2.0	7.4	2.9			
3	Limestone shale	0.25	1.6	10.2	-	-	-	-			
4	Limestone shale	0.4	0.8	4.1	-	-	-	-			
5	Clause 810 over limestone shale	0.2+0.25	-	-	-	-	-	-			
6	Clause 810 over limestone shale	0.1+0.25	-	-	-	-	-	-			

Figure 1.

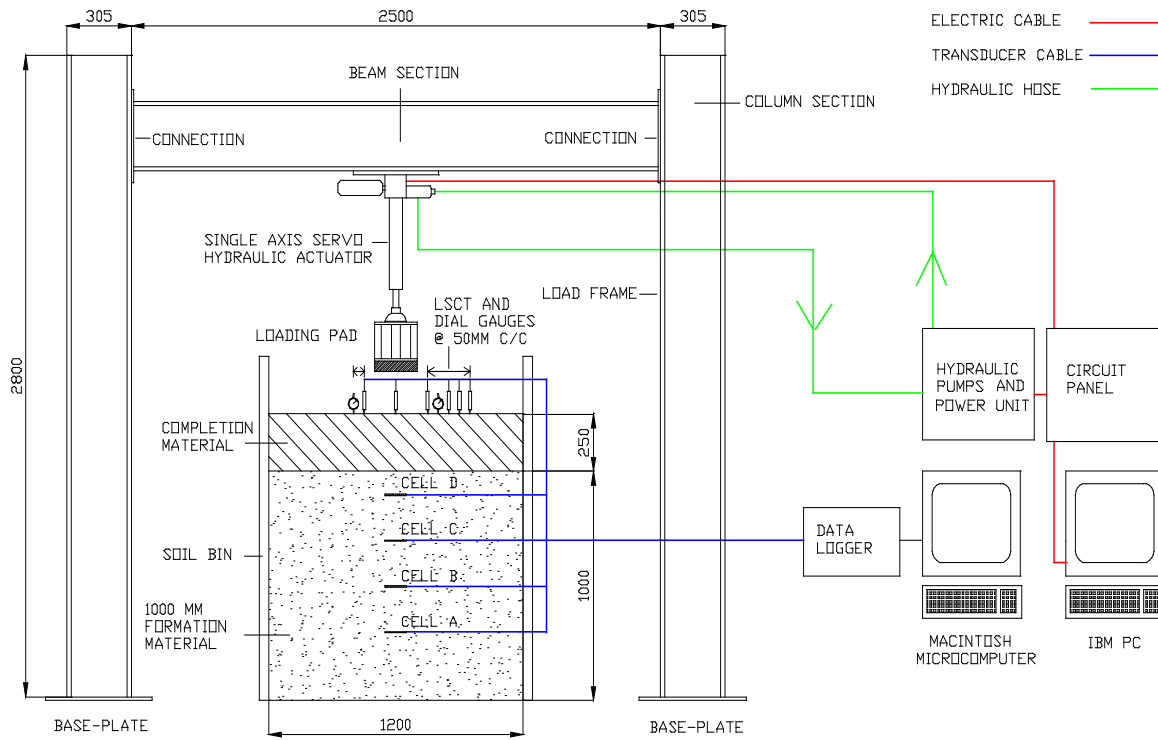




Figure 2.

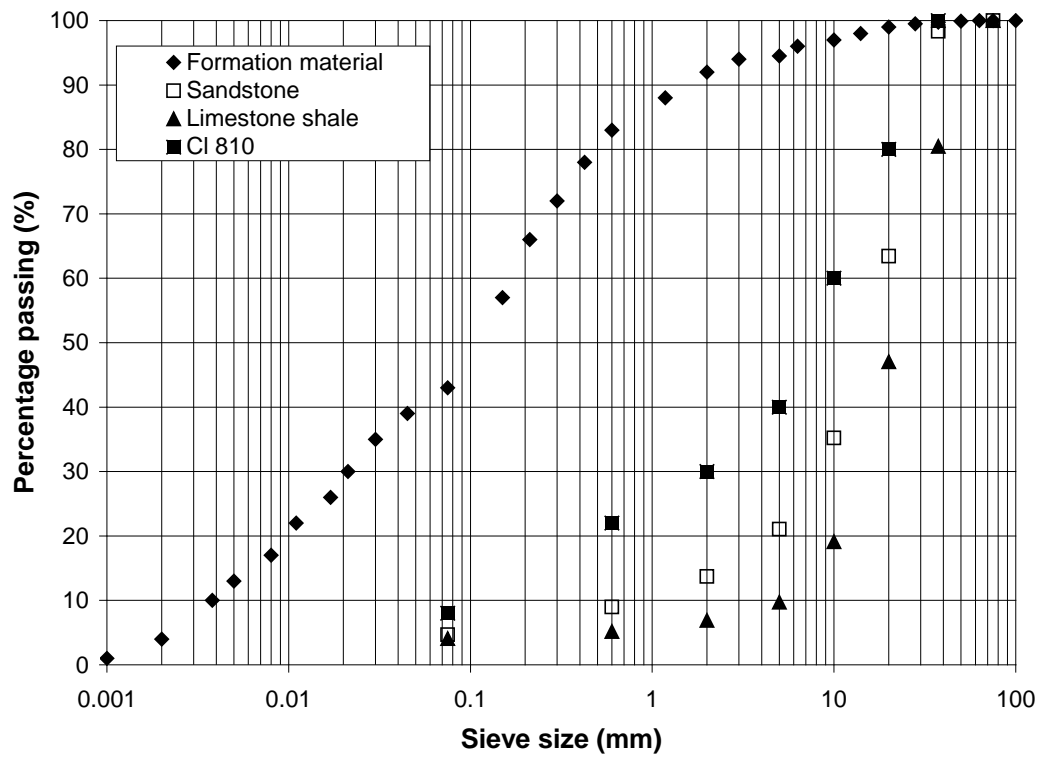


Figure 3.

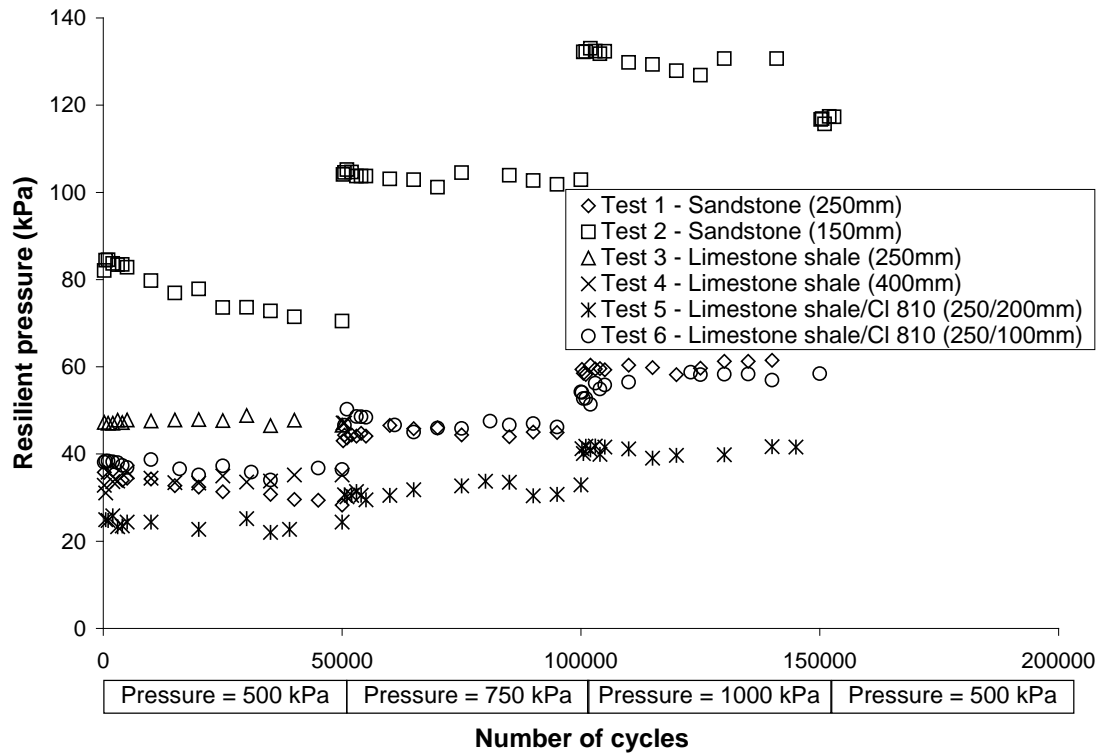


Figure 4.

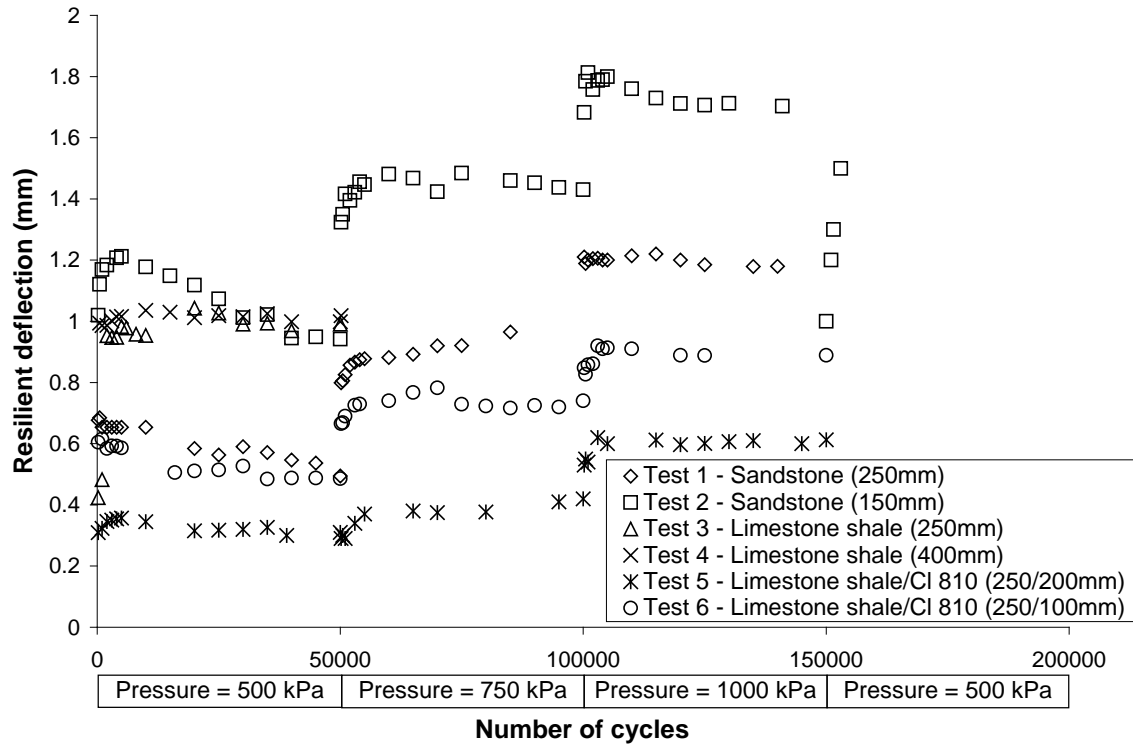


Figure 5.

